

## ANALYSIS OF TRITIUM TRANSPORT MECHANISMS AT THE SURFACE OF LITHIUM CERAMICS

Alya Badawi, A. René Raffray and Mohamed A. Abdou  
Mechanical, Aerospace and Nuclear Engineering Department,  
University of California, Los Angeles, CA 90024  
(310)206-1228

### ABSTRACT

An analysis was made of the surface fluxes of hydrogen species in order to determine the activation energies which affect the bulk and surface inventories in a lithium ceramic. It was found that in the absence of protium, Sievert Law is obeyed and the concentration depends on  $\sqrt{P_{T2}}$ . However, in the presence of protium, the concentration depends on  $P_{HT}$ . The bulk and surface concentrations were found to depend on a combination of all four surface energies in the activation energy of solution and the heat of adsorption.

### I. INTRODUCTION

Accurate calculation of the tritium inventory in a fusion reactor blanket requires, among other things, the specification of various fluxes of different hydrogen species entering and leaving the surface of the breeder. These fluxes are important because they control the release of the tritium from the bulk breeder, in addition to controlling the amount of tritium on the surface of the material and in the pore system<sup>1</sup>. In order to determine the surface fluxes different activation energies need to be known. Unfortunately, there are very limited data on the activation energies of lithium ceramics.

In this paper, the fluxes on the lithium ceramic surface are defined and an analysis is made to determine the activation energies which most affect the bulk and surface inventories in the solid breeder. In the absence of fundamental property data, the results of this parametric study would help to estimate values of the activation energies of the different surface processes to be used as input in tritium modeling codes such as MISTRAL<sup>1</sup> for experimental data or blanket analysis.

### II. DEFINITION OF SURFACE FLUXES

Fig. 1 shows the different fluxes entering and leaving the surface. From this figure, four fluxes (at/m<sup>2</sup> s) can be identified<sup>1</sup>:

1. A flux entering the surface from the bulk side,  $R_{\beta}$ , defined as

$$R_{\beta} = k_{\beta} C_{bs} (1 - \theta) \exp(-E_{\beta}/RT) \quad (1)$$

$$k_{\beta} = \frac{10^{13}}{\sqrt{N_s}} \frac{3}{S_{BET} r_g \rho} \quad (2)$$

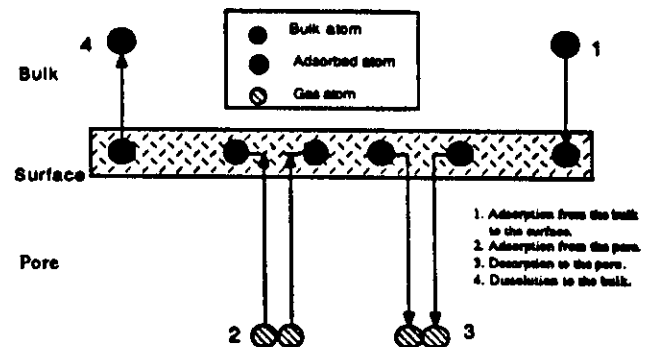


Fig. 1. Schematic diagram of the different fluxes entering and leaving the surface.

where  $C_{bs}$  is the tritium concentration in the bulk just below the surface,  $\theta$  is the surface coverage,  $E_{\beta}$  is the activation energy for adsorption from the bulk to the surface,  $R$  is the universal gas constant,  $T$  is the temperature,  $N_s$  is the number of sites on the surface of the breeder,  $S_{BET}$  is the specific surface area,  $\rho$  is the breeder density, and  $r_g$  is the breeder grain radius. The factor  $(3/S_{BET} r_g \rho)$  is used to convert the atom flux from a grain surface area basis to the actual surface area basis.

2. A flux leaving the surface to the pore, or the desorption flux,  $R_{des}$

$$R_{des} = k_{des} \theta^2 \exp(-2E_{des}/RT) \quad (3)$$

$$k_{des} = \frac{R N_s z T}{A_v h} \quad (4)$$

$E_{des}$  is the activation energy for desorption,  $z$  is the number of adjacent sites to each atom,  $A_v$  is Avogadro's number, and  $h$  is Planck's constant.

3. A flux entering the surface from the pore, or the adsorption flux,  $R_{ads}$

$$R_{ads} = k_{ads} C_p (1 - \theta)^2 \exp(-2E_{ads}/RT) \quad (5)$$

$$k_{ads} = \frac{\sigma z}{\sqrt{8 \times 10^{-3} \pi}} \sqrt{\frac{RT}{M}} \quad (6)$$

$C_p$  is the concentration in the pore at the surface,  $E_{ads}$  is the

adsorption activation energy,  $\sigma$  is the sticking coefficient, and  $M$  is the molecular weight of the adsorbing species. The factors  $(1 - \theta)^2$  and  $\theta^2$  are included in the adsorption flux

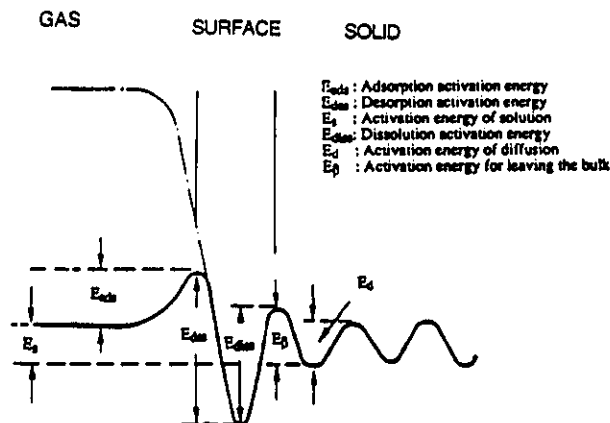


Fig. 2. Potential energy diagram for atomic and molecular hydrogen at the surface.

and desorption flux, respectively, in addition to the use of twice the activation energies, in accordance with Ref. [2]. This follows from the assumption of the activation energy being associated with one surface site. For adsorption the hydrogen molecule is assumed to dissociate into two atoms each requiring a surface site on which to adsorb. Conversely for desorption, atoms or radicals from two surface sites combine and desorb as a molecule.

4. A dissolution flux,  $R_{diss}$ , denoting the atoms entering the bulk from the surface. It is defined as

$$R_{diss} = k_{diss} \theta \exp(-E_{diss}/RT) \quad (7)$$

By analogy to  $k_{des}$ ,

$$k_{diss} = \frac{R N_s z T}{A_v h} \quad (8)$$

$E_{diss}$  is the activation energy for dissolution.

Fig. 2 shows the relation between the activation energies. From this figure, it can be shown that<sup>2</sup>

$$E_s = (E_{diss} - E_\beta) + (E_{ads} - E_{des}) \quad (9)$$

where  $E_s$  is the activation energy of solution, defined as the energy of the hydrogen atom in the bulk relative to that in the gas phase.

The four fluxes are related to the concentration in the bulk and to each other through the following relation<sup>1</sup>

$$D_b \left( \frac{\partial C_b}{\partial x} \right)_{\text{surface}} = R_\beta - R_{diss} \quad (10)$$

and

$$N_s \frac{d\theta}{dt} = R_\beta - R_{diss} + R_{ads} - R_{des} \quad (11)$$

where  $D_b$  is the diffusion coefficient in the bulk,  $x$  is the coordinate along the bulk diffusion path and  $C_b$  is the tritium concentration in the bulk

### III. EFFECT OF ACTIVATION ENERGIES ON SURFACE AND BULK INVENTORIES

#### III.A. No H<sub>2</sub> In The Purge

In order to understand how the surface fluxes affect the bulk as well as the surface inventory, we start by the simplest case which corresponds to the experiments for measuring the solubility. Consider a steady state with no tritium generation and no protium in the purge gas. Since there is only tritium on the surface, the tritium surface coverage,  $\theta_T$ , will be equal to the total surface coverage,  $\theta$ . At steady state,  $R_\beta = R_{diss}$  and  $R_{ads} = R_{des}$ . Assuming  $\theta$  is  $\ll 1$ , from eqs. (1), (3), (5) and (7), we get:

$$C_{bs} = \frac{k_{diss}}{k_\beta} \theta \exp [(E_\beta - E_{diss})/RT] \quad (12)$$

$$\theta = \sqrt{\frac{k_{ads}}{k_{des}}} \sqrt{C_{PT_2}} \exp [(E_{des} - E_{ads})/RT] \quad (13)$$

The quantity  $(E_{des} - E_{ads})$  is defined as  $Q$ , the heat of adsorption. Substituting (13) and (9) in (12) we get:

$$C_{bs} = \frac{k_{diss}}{k_\beta} \sqrt{\frac{k_{ads}}{k_{des}}} \sqrt{C_{PT_2}} \exp (-E_s/RT) \quad (17)$$

It can be seen from eq. (13) that the surface coverage increases with increasing  $Q$ . Also, from the square root dependence on  $C_{PT_2}$ ,  $\theta$  will depend on  $\sqrt{P_{T_2}}$ , where  $P_{T_2}$  is the tritium partial pressure in the pore. Therefore, the surface and surface driven bulk inventories,  $I_s$  and  $I_{bs}$ , which are proportional to  $\theta$  and  $C_{bs}$ , respectively, can be written as

$$I_s = A_1 \exp (Q/RT) \sqrt{P_{T_2}} \quad (15)$$

$$I_{bs} = A_2 \exp (-E_s/RT) \sqrt{P_{T_2}} \quad (16)$$

where  $A_1$  and  $A_2$  are constants determined by the temperature and microstructure of the material. The bulk concentration was assumed to be uniform in eq. (16), which is Sievert's Law in which the concentration in the bulk is proportional to the square root of the pressure.

Calculations can be taken a step further by considering the case with tritium generation in the bulk. At steady state:

$$R_\beta - R_{diss} = g \quad (17)$$

$$R_{des} - R_{ads} = g \quad (18)$$

where  $g$  is the effective tritium atom generation rate in the bulk per unit surface area. Assuming  $\theta \ll 1$ , from eqs. (17) and (18) we get:

$$C_{bs} = \frac{k_{diss}}{k_\beta} \theta \exp [(E_\beta - E_{diss})/RT] + \frac{g}{k_\beta} \exp (E_\beta/RT) \quad (19)$$

$$\theta = \sqrt{\frac{k_{ads}}{k_{des}} C_{PT2} + \frac{g}{2k_{des}} \exp(2E_{ads}/RT)} \exp(Q/RT) \quad (20)$$

substituting for  $\theta$  in (19) we get

$$C_{bs} = \frac{k_{diss}}{k_{\beta}} \left( \frac{k_{ads}}{k_{des}} C_{PT2} + \frac{g}{2k_{des}} \exp(2E_{ads}/RT) \right)^{1/2} \exp(-E_s/RT) + \frac{g}{k_{\beta}} \exp(E_{\beta}/RT) \quad (21)$$

In this case an additional term emerges in both eqs. (20) and (21). This term increases with  $g$  and  $E_{ads}$ , and indicates that the coverage is increasingly dependent on the tritium generation rate and hence on the flux from the bulk as the adsorption activation energy increases and, hence, the flux from the pore decreases. In addition, a second term emerges in eq. (21) for  $C_{bs}$ . This term increases with  $g$  and  $E_{\beta}$ , and can be explained by noting that as  $E_{\beta}$  increases, a larger bulk concentration driven by  $g$  is required to keep the flux from the bulk to the surface in equilibrium with the generation rate at steady state.

### III. B. H<sub>2</sub> In The Purge

Experiments have shown that the addition of H<sub>2</sub> to the purge gas enhances the release of tritium from the solid breeder materials. This is thought to be due to the replacement of the protium to the tritium on the surface of the material<sup>3</sup>. Hence the addition of protium is expected to influence the surface fluxes.

Consider a steady state case with no tritium generation. Equating  $R_{\beta}$  to  $R_{diss}$  for tritium:

$$C_{bs} = \theta_T \frac{k_{diss}}{k_{\beta}} \exp((E_{\beta} - E_{diss})/RT) \quad (22)$$

Equating  $R_{ads}$  to  $R_{des}$  for tritium, assuming  $\theta \ll 1$  and  $C_{PT2} \ll C_{PHT}$ :

$$\theta_T \theta = \frac{k_{adsHT}}{2k_{des}} C_{PHT} \exp[2(E_{des} - E_{ads})/RT] \quad (23)$$

Note that although  $k_{des}$  is the same for both species,  $k_{ads}$  is not, since it depends on the molecular weight.

Equating  $R_{ads}$  to  $R_{des}$  for protium, assuming that  $\theta_T \ll \theta_H$  and  $C_{PHT} \ll C_{PH2}$ :

$$\theta_H = \sqrt{\frac{k_{adsH2} C_{PH2}}{k_{des}}} \exp(Q/RT) \quad (24)$$

substituting for  $\theta$  in (23), assuming  $\theta \sim \theta_H$  we get:

$$\theta_T = \frac{k_{adsHT}}{2\sqrt{k_{adsHT} k_{des}}} \frac{C_{PHT}}{\sqrt{C_{PH2}}} \exp((2E_{des} - E_{ads})/RT) \quad (25)$$

Substituting for  $\theta$  in eq. (23), we get

$$C_{bs} = \frac{k_{adsHT}}{2\sqrt{k_{adsH2} k_{des}}} \frac{k_{diss}}{k_{\beta}} \frac{C_{PHT}}{\sqrt{C_{PH2}}} \exp(-E_s/RT) \quad (26)$$

Eqs. (24)-(26) show some interesting points:

1. The hydrogen coverage is a function of  $\sqrt{C_{PH2}}$ . However, the tritium surface coverage is a function of  $C_{PHT}/\sqrt{C_{PH2}}$ .
2. The tritium coverage is a function of the exponential of the heat of adsorption for both cases with and without protium addition. However, the preexponential constants are different.
3. The surface-driven bulk inventory is a function of the exponential of the activation energy of solution for both cases with and without protium. However, the preexponential constants are different, and while  $C_{bs}$  is a function of  $\sqrt{C_{PT2}}$  for the case without protium, it is a function of  $C_{PHT}/\sqrt{C_{PH2}}$  for the case with protium.

At steady state, when tritium is generated and H<sub>2</sub> is present in the purge gas,  $C_{bs}$  and  $\theta_T$  are given by<sup>4</sup>

$$\theta_T = \frac{1}{2\sqrt{k_{adsH2} k_{des}}} \frac{1}{\sqrt{C_{PH2}}} \frac{1}{(k_{adsHT} C_{PHT} + g \exp(2E_{ads}/RT)) \exp(Q/RT)} \quad (27)$$

$$C_{bs} = \left\{ \frac{k_{adsHT} C_{PHT} + g \exp(2E_{ads}/RT)}{k_{diss}} \right\} \frac{1}{2k_{\beta} \sqrt{k_{adsH2} k_{des}}} \frac{1}{\sqrt{C_{PH2}}} \exp(-E_s/RT) + \frac{g}{k_{\beta}} \exp(E_{\beta}/RT) \quad (28)$$

## IV. ANALYSIS OF THE RESULTS

To determine the magnitude of  $E_s$ ,  $Q$ ,  $E_{ads}$  and  $E_{\beta}$  at which they become important in determining  $\theta$  and  $C_{bs}$ , all the constants need to be calculated. In order to get an idea of the relation between inventories and activation energies, the values obtained from the MOZART experiment for a Li<sub>2</sub>O sample were used<sup>5</sup>, as shown in Table I, together with four different protium concentrations in the purge: 0%, 0.01%, 0.1% and 1%. In addition, it is assumed that  $C_p$  is constant in the pore. The numerical results obtained below should be regarded in the context of the above assumptions and are mostly intended in identifying major trends. For confirmation purposes, calculations were also done using MISTRAL for the same cases by setting artificially high values for the bulk and pore diffusion coefficients in order to obtain results compatible with the present analysis.

TABLE I  
Data from MOZART Experiment for Li<sub>2</sub>O Sample

Porosity	20%
Sample Diameter (m)	8 x 10 <sup>-3</sup>
Sample Length (m)	0.03
Purge Gas Pressure (Pa)	1.6 x 10 <sup>5</sup>
Purge Gas Flow Rate (l/h)	2.84
Tritium Generation Rate (at/m <sup>3</sup> s)	1.01 x 10 <sup>19</sup>
Breeder Volume (m <sup>3</sup> )	1.509 x 10 <sup>-6</sup>
Grain Volume (m <sup>3</sup> )	2.14 x 10 <sup>-15</sup>
Temperature (K)	923

The values of  $C_{PT2}$  and  $C_{PHT}$  are determined by the purge flow rate as well as the diffusion coefficient in the pore. If we assume that tritium diffuses very rapidly in the pore then the concentration of tritium in the pore can be assumed uniform and equal to the tritium concentration in the purge. Thus, at steady state, the total concentration of tritium atoms in the pore,  $C_{PT}$  would vary from zero to a maximum depending on the purge flow rate and tritium production rate. In the case of  $C_{PT}$  equals zero, the above equations are not valid, since there is no adsorption flux in this case. However, rederiving the equations, it was found that eqs. (20), (21), (25) and (26) can be used with  $C_{PT}=0^4$ .

For the purpose of analysis, three values of  $C_{PT} = 0, 1.34 \times 10^{15}$  and  $1.55 \times 10^{19}$  at/m<sup>3</sup>, corresponding to minimum, maximum and intermediate pore concentrations, were chosen<sup>4</sup>.

The results are summarized in Figs 3 - 7. Figs 3 and 4 show the dependence of  $\theta_T$  on  $E_{ads}$  for the three values of  $C_{PT}$  in the absence and presence of protium, respectively. Although  $Q$  is not known for most lithium ceramics, it is expected to be lower in the presence of protium, due to the increase in the surface coverage. For the cases with pure helium,  $Q$  was chosen to be 60 kJ/mol. For the cases with protium,  $Q$  was chosen to be 30 kJ/mol. Note that changing the values of  $Q$  will shift the curves in the vertical direction without changing the profiles. From Fig. 3, there is a threshold energy, the value of which depends on the tritium concentration in the pore, above which the tritium surface coverage increases exponentially. This threshold energy is 0 for  $C_{PT} = 0$ , is 25 kJ/mol for  $C_{PT} = 1.34 \times 10^{15}$  and is 55 kJ/mol for  $C_{PT} = 1.55 \times 10^{19}$  at/m<sup>3</sup>. It should be noted that when a regular pore diffusion coefficient was used in MISTRAL, the dependence of  $\theta_T$  on  $E_{ads}$  did not start until about 40 kJ/mol.

From Fig. 4, the increase of protium content in the purge shifted the curves downward without changing the profiles. Therefore, only one case (with 1% H<sub>2</sub>) was shown in all the figures. The ratio  $\theta_T/\theta_H$  was always  $< 10^{-4}$ , and, therefore, the assumption that  $\theta_T \ll \theta_H$  that was used in the derivations is valid. Fig. 4 shows a similar behavior to Fig. 3. However, the threshold energy of adsorption is higher in this case than the case of pure helium. In addition, the presence of protium decreases  $\theta_T$  for the same  $C_{PT}$  and  $E_{ads}$ .

The effect of  $E_{ads}$  on the surface-driven bulk inventory,  $I_{bs}$ , which is proportional to  $C_{bs}$ , was found to exhibit a similar behavior to Figs. 3 and 4<sup>4</sup>. There is a threshold energy of adsorption that increases with increasing  $C_{PT}$ , above which  $I_{bs}$  increases exponentially. However, in the presence of protium and  $C_{PT} = 0$  the threshold energy was equal to 45 kJ/mol and not 0 as in the case of the surface coverage (Fig. 4). This difference is due to the presence of an additional term in the case of  $C_{bs}$ , that depends on  $E_{\beta}$  and  $g$  (eq. (28)).

The effect of  $Q$  on  $\theta$  (or  $I_s$ ) is shown in Fig. 5 for  $E_{ads} = 15$  kJ/mol and  $C_{PT} = 1.34 \times 10^{15}$  at/m<sup>3</sup>. The surface coverage increases exponentially with the heat of adsorption. However, the results are not valid at high coverage, since in the calculations certain terms were neglected when  $\theta$  was assumed to be  $\ll 1$ . Again the addition of protium is seen to

decrease the tritium surface coverage for the same heat of adsorption. The decrease in  $\theta_T$  when changing from 0 to 1% H<sub>2</sub> in the purge is more pronounced than it appears, since typically  $Q$  would also decrease and thus the final  $\theta_T$  value would be even lower. For  $C_{PT} = 0$  and  $C_{PT} = 1.55 \times 10^{19}$  at/m<sup>3</sup>, the same patterns were observed.

Fig. 6 shows the effect of  $E_s$  on  $I_{bs}$  for  $E_{ads} = 15$  kJ/mol,  $E_{\beta} = 100$  kJ/mol and  $C_{PT} = 1.34 \times 10^{15}$  at/m<sup>3</sup>. As  $E_s$  increases  $I_{bs}$  decreases exponentially for all the cases.

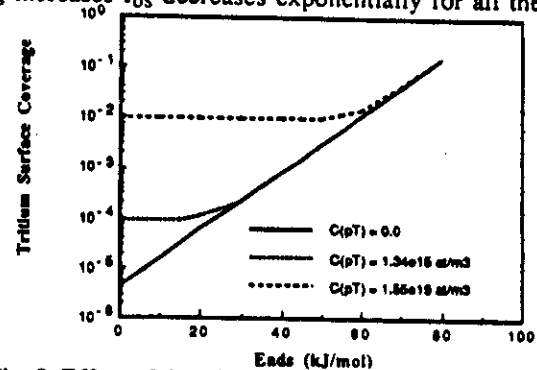


Fig. 3. Effect of the adsorption activation energy on the surface coverage (pure He,  $Q = 60$  kJ/mol).

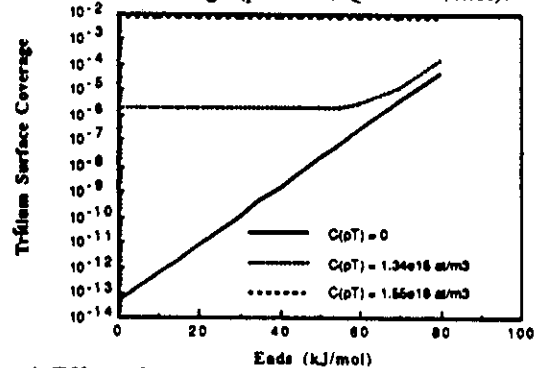


Fig. 4. Effect of the Adsorption Activation Energy on the Surface Coverage (He + 1% H<sub>2</sub>,  $Q = 30$  kJ/mol)

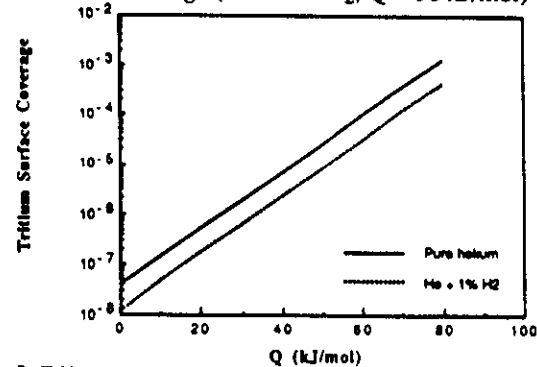


Fig. 5. Effect of the heat of adsorption on the tritium surface coverage ( $C_{PT} = 1.34 \times 10^{15}$  at/m<sup>3</sup>,  $E_{ads} = 15$  kJ/mol).

This was also confirmed using MISTRAL with values of  $E_s$  between 0 and 25 kJ/mol. For values of  $E_s > 100$  kJ/mol, the change in the surface-driven bulk inventory becomes insignificant. It should be noted that  $E_s$  is not used as an input in the MISTRAL code. Instead, the values of  $E_{\beta}$ ,  $E_{diss}$ ,  $E_{ads}$ , and  $E_{des}$  are used. Therefore, in addition to showing that  $I_{bs}$  changes with  $E_s$ , the code also showed that  $I_{bs}$  does not change by changing any 2 - 4 activation

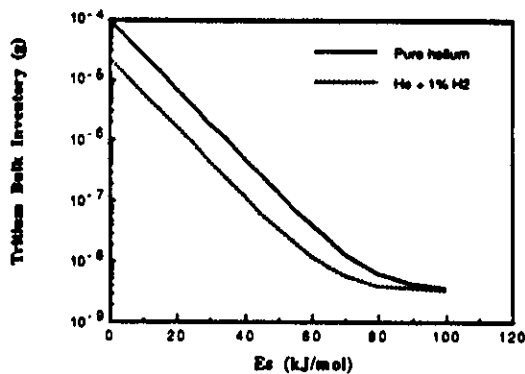


Fig. 6. Effect of the activation energy of solution on the surface-driven bulk inventory ( $C_{PT} = 1.34 \times 10^{15} \text{ at/m}^3$ ,  $E_{ads} = 15 \text{ kJ/mol}$ ,  $E_{\beta} = 100 \text{ kJ/mol}$ ).

energies simultaneously. Addition of protium to the purge leads to lower values of  $I_{bs}$  but shows dependence on  $E_s$  as compared to the purge helium purge case. Again, for  $E_s$  values greater than about 100 kJ/mol, the change in  $I_{bs}$  is negligible. For  $C_{PT} = 0$  and  $1.55 \times 10^{19} \text{ at/m}^3$ , the same patterns was observed.

Figs. 7 shows the effect of  $E_{\beta}$  on  $I_{bs}$  for  $E_{ads} = 15 \text{ kJ/mol}$  and  $C_{PT} = 0, 1.34 \times 10^{15}$  and  $1.55 \times 10^{19} \text{ at/m}^3$ . For pure helium, the threshold energy of  $E_{\beta}$  increases with  $C_{PT}$ . When protium is present, the threshold energy still increases with  $C_{PT}$ . However, it is less for the same  $C_{PT}$ . This is the opposite of the effect of protium on the threshold activation energy of adsorption (Figs. 3 and 4).

## V. CONCLUSIONS

From the above results, the following observations can be made:

1. The addition of protium will affect both the bulk as well as the surface inventories.
2. Without protium in the purge, the surface-driven bulk concentration depends on  $\sqrt{P_{T2}}$ . When protium is present in the purge, the surface-driven bulk concentration depends on PHT.
3. The adsorption activation energy,  $E_{ads}$ , affects the surface coverage and the bulk inventory. The threshold energy at which this effect becomes important increases with increasing the tritium concentration in the pore and/or adding protium to the purge. When  $C_{PT} = 0$ , both  $\theta_T$  and  $I_{bs}$  increase exponentially with  $E_{ads}$ , with no threshold energy. However, in a realistic situation,  $C_{PT}$  is expected to be more than  $10^{15} \text{ at/m}^3$ . At this value, for the  $\text{Li}_2\text{O}$  example considered, the threshold activation energy will be  $> 25 \text{ kJ/mol}$ . Although the adsorption energy is not known for most lithium ceramics, it is usually small for metals<sup>2</sup> and is between 3 - 15 kJ/mol for  $\text{LiAlO}_2$ , between 200 and 500°C<sup>6</sup>. Therefore, in this case, it is not expected to play an important role in determining the inventories.
4. The bulk inventory changes exponentially for  $E_s$  between 0 and 100 kJ/mol. As mentioned earlier, the activation energy of solution was estimated by Katsuta<sup>7</sup> as 16 kJ/mol for  $\text{H}_2$  in  $\text{Li}_2\text{O}$  and 19 kJ/mol for  $\text{D}_2$  and was estimated by Glugla<sup>8</sup> for  $\text{H}_2$  in  $\text{Li}_2\text{SiO}_3$  as 29 kJ/mol. For an HT mixture, Kudo and O'hira<sup>9</sup> found  $E_s$  to be 24 - 25 kJ/mol in  $\text{Li}_2\text{O}$ . Thus the value of  $E_s$  is a key factor in determining

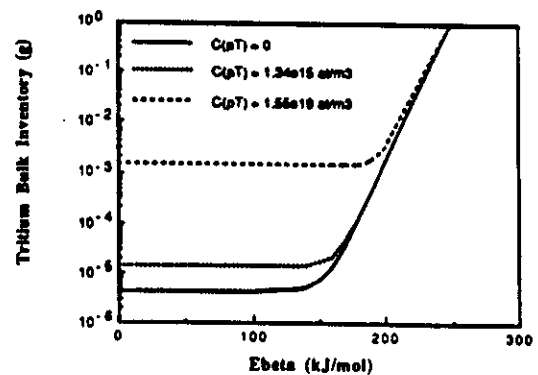


Fig. 7. Effect of  $E_{\beta}$  on the surface-driven bulk inventory (pure He,  $E_{ads} = 15 \text{ kJ/mol}$ ,  $E_s = 15 \text{ kJ/mol}$ ).

the surface-driven bulk inventory, since it lies in the range over which the inventory changes exponentially.

5. The surface-driven bulk inventory changes exponentially with  $E_{\beta}$ . The threshold energy at which  $E_{\beta}$  becomes important also increases with  $C_{PT}$ . However, it decreases with the addition of protium. For  $C_{PT} = 0$  and protium present, the threshold energy = 30 kJ/mol for the  $\text{Li}_2\text{O}$  example considered. In a realistic situation, however, where  $C_{PT}$  has a finite value, the threshold energy is expected to be  $> 120 \text{ kJ/mol}$ . This seems high for  $E_{\beta}$  which for this case is, thus, not expected to play a major role in determining surface and surface-driven bulk inventory.

6. It is interesting to note that individually,  $E_{ads}$  and  $E_{\beta}$  are not expected to significantly affect surface-dependent inventories, provided their values do not exceed their corresponding thresholds based on the material considered (about 25 and 120 kJ/mol, respectively in the example case considered). It is the combination of all four surface energies in  $E_s$  and of  $E_{des}$  and  $E_{ads}$  in  $Q$  which are the key factors in determining surface-dependent inventories at steady state.

## VI. REFERENCES

1. G. Federici, Ph.D. Dissertation, University of California at Los Angeles (October 1989), also G. Federici, A.R. Raffray and M.A. Abdou, "MISTRAL: A Comprehensive Model for Tritium Transport in Lithium-Base Ceramics Part I: Theory and Description of Model Capabilities," *J. Nucl. Mater.*, 173, 185(1990).
2. M.A. Pick and K. Sonnenberg, "A Model for Atomic Hydrogen-Metal Interactions - Application to Recycling, Recombination and Permeation," *J. Nucl. Mater.*, 131, 208 (1985).
3. A.K. Fischer and C.E. Johnson, "Thermochemical Comparison of the Effectiveness of Protium Purging of Fusion Breeders," *Fusion Technol.*, 8, 871 (1985).
4. A. Badawi and A.R. Raffray, "Analysis of Surface Fluxes of Hydrogen Species in Lithium Ceramics," UCLA-FNT-50, UCLA Report (Dec. 1991).
5. M. Bricc, "The MOZART Experiment - Tritium Extraction from  $\text{Li}_2\text{O}$ ,  $\text{LiAlO}_2$ ,  $\text{Li}_2\text{ZrO}_3$ ," CEA Report.
6. A.K. Fischer and C.E. Johnson, "Adsorption, Dissolution and Desorption Characteristics of  $\text{LiAlO}_2\text{-H}_2\text{O(g)}$  System," DOE/ER-0313, Semiannual Progress Report, 419 (May 1989).
7. H. Katsuta, S. Konishi and H. Yoshida, "Solubility and Diffusivity of Hydrogen in  $\text{Li}_2\text{O}$ ," *J. Nucl. Mater.*, 116, 244 (1983).
8. M. Glugla, K.H. Simon and R.-D. Penzhorn, "The Solubility of Hydrogen in Lithium Metasilicate," *J. Nucl. Mater.*, 155-157, 513 (1988).
9. S. O'hira, T. Hayashi, K. Okuno and H. Kudo, "Tritium Dissolution in and Release from  $\text{Li}_2\text{O}$ ," *Fusion Eng. Design*, 8,335 (1989).